

## Divertor power handling assessment for baseline scenario operation in JET in preparation for the ILW

I Nunes<sup>1</sup>, P J Lomas<sup>2</sup>, G Saibene<sup>3</sup>, T Eich<sup>4</sup>, G Arnoux<sup>2</sup>, H Thomsen<sup>5</sup>, E de la Luna<sup>6</sup>  
and the JET EFDA contributors\*

<sup>1</sup>Instituto de Plasmas e Fusão Nuclear, Associação EURATOM-IST, Lisboa, Portugal

<sup>2</sup>Culham Science Centre, EURATOM-UKAEA Association, Abingdon OX14 3DB, UK

<sup>3</sup>Fusion for Energy, Barcelona, Spain

<sup>4</sup>Max Planck Institut für Plasma Physik, EURATOM Association, Germany

<sup>5</sup>Max-Planck-Institut für Plasmaphysik, EURATOM-Assoziatiön, Greifswald, Germany

<sup>6</sup>Laboratorio Nacional de Fusión, Asociación EURATOM-CIEMAT, Madrid, Spain

\*See Appendix of F Romanelli et al., Fusion Energy 2008 (Proc. 22nd Int Conf Geneva, 2008) IAEA, (2008)

### 1. Introduction

The ITER-like Wall (ILW) project in JET is replacing the currently used plasma facing components (PFCs), made with Carbon-Fibre Composite (CFC) by Be (wall) and W (divertor) for operation in 2011. This to mimic the proposed PFCs for the DT operational phase of ITER. The new W divertor is planned to have a central divertor target plate (tile 5 in figure 1(a)) made of solid W while the rest of the divertor target tiles are W coated CFC tiles [1]. The bulk W row is segmented poloidally into 4 stacks per tile and toroidally in 24 lamellae per stack to minimise the eddy current loads.

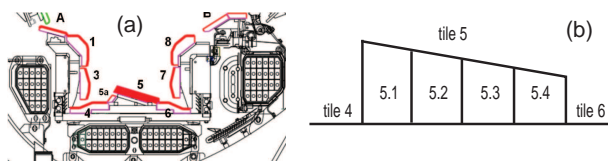


Figure 1: (a) Poloidal cross-section of the planned W divertor at JET and (b) present tile 5 divided into 4 stacks.

The tile segmentation and the support structure determines the power and energy limits on the divertor [2] defining the tiles power and energy handling and therefore the level of additional heating and pulse length. Various techniques to reduce both continuous and transient power load on the divertor are being explored at JET, such as ELM mitigation by using resonant magnetic perturbation [3], vertical kicks to control the ELM frequency [4] and nitrogen seeding to increase the plasma radiated power [5,6]. The tile design gives rise to surface temperature limits (for the W coating) as well as bulk temperature limits (for the tile fixings). Recently, experiments have been carried out at JET to test the sweep amplitude necessary to reduce the power and energy loads to the divertor tiles while keeping the same H-mode performance as the reference non-swept plasma, for low and high triangularity configurations, similar to those carried out in 1991/1992 [7].

### 2. Experimental set-up

The present tile on position 5 (tile 5) is a solid CFC tile. For the analysis presented in this paper, the length of this tile was divided into 4 to mimic the 4 stacks of the foreseen bulk W as shown in figure 1(b). A plasma with a fixed outer strike position on tile 5, stack 3 (static) at  $I_p=2.5\text{MA}$ ,  $B_T=2.2\text{T}$  with 15MW of additional heating for 8.5s (13MW of NBI and 2MW of ICRH) is used as a reference plasma. This reference plasma has a confinement enhancement factor  $H_{98} = 1.06$  (averaged over a steady state phase) and normalised beta of 1.8-1.9 at  $q_{95}=3$ . Various sweep amplitudes were tested at a sweeping frequency of 4Hz: Sweep 1 between tiles 6 and 5.4 (one stack), sweep 2 between tiles 6

and 5.3 (two stacks) and sweep 3 between tiles 5.4 and 5.2 (two stacks on tile 5). Please note that sweeps 1 and 2 use part of tile 6 which is closer to the opening of the divertor cryo pump, providing better pumping. With the ILW, the use of tile 6 will be limited because of the lifetime restriction of the W coating (thin coating). The plasma shape was

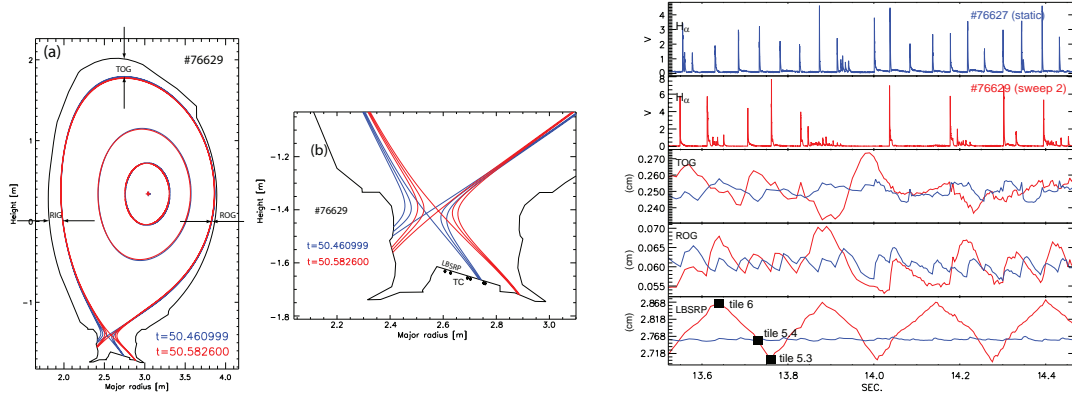


Figure 2: (a) Plasma shapes (low  $\delta$ ) at the extreme positions of the largest sweep tested (sweep 2, between tile 6 and tile 5), (b) detail of the divertor (c) time evolution of the D $\alpha$  emission, top gap, outer gap, inner gap and strike point position.

tuned such that the core plasma shape stays approximately constant while sweeping the outer strike points (figure 2). For these experiments two magnetic configurations were used; one low triangularity configuration with  $\delta_{avg} = 0.27$  ( $\delta_{upper}=0.17$  and  $\delta_{lower}=0.37$ ), and a high triangularity configuration with  $\delta_{avg} = 0.42$  ( $\delta_{upper}=0.44$  and  $\delta_{lower}=0.4$ ). As shown in figure 2(b), for the largest sweep amplitude used,  $\delta_{lower}$  varies  $\approx 14\%$  for the low triangularity configuration and  $\approx 10\%$  for the high triangularity configuration. Moreover, the inner (RIG), top (TOG) and outer (ROG) gaps vary less than 2 cm ( $\leq 3\%$  of the plasma minor radius) during the sweep. It is observed that as the sweep amplitude increases the ELMs become more compound. This seems to be correlated with the increase of ROG (decrease in RIG) coupled with the sweep (figure 2(c)). A possible explanation is that the sweep will shrink the plasma column by moving ROG and TOG which can change the edge current causing the compound behaviour of the ELMs.

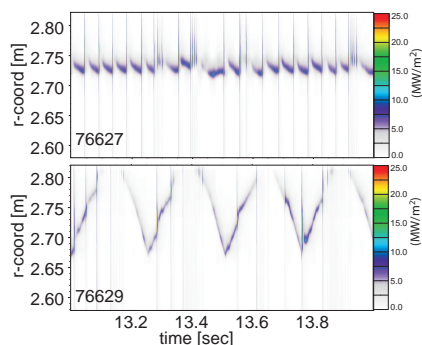


Figure 3: Heatflux measurements with IR.

### 3. Divertor tile surface and bulk temperature

The analysis of the surface temperature of the divertor tiles uses infra-red (FLIR ATS) measurements with high spatial (2mm) and temporal (up to 35  $\mu$ s) resolution [8]. An example of the heat flux near the outer strike is depicted in figure 3. The static and the swept configurations have a similar heatflux to the target, up to 10MW/m $^2$  in between ELMs. For the swept configuration this power is distributed over a region of  $\approx 16$ cm, which is 4 times larger than the typical scrape-off layer e-folding length. Figure 4(a) compares the evolution of the surface temperature of the divertor tile for the static case (red) and the sweep case (blue) for sweep 2. The temperature evolution on the four (virtual) sections of tile 5 and the sweep amplitude of the outer strike point during 8s of additional heating is shown in figure 4(a). The baseline temperature (inter-ELM) increases from  $\approx 300^\circ$ C

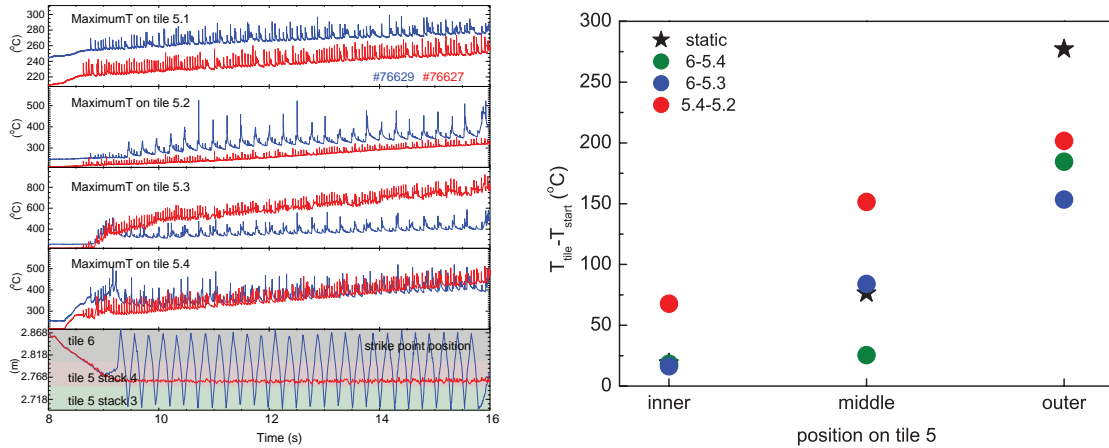


Figure 4: Time traces of tile 5 surface temperature for the 4 (virtual) stacks measured by IR and (b) peak temperature on tile 5 measured by the thermocouples for all cases.

to  $\approx 800^\circ\text{C}$  on tile 5.3 for the unswept case whilst for the swept case the surface temperature rises from  $\approx 300^\circ\text{C}$  to only  $\approx 400^\circ\text{C}$ , a dramatic reduction of the temperature excursion. Section 5.4 has a similar temperature excursion indicating a good power distribution during the sweep. For these plasma discharges, a typical ELM crash measured in stored energy is about 400kJ. The peak temperature during these ELMs on any section of tile 5 stays at or below  $600^\circ\text{C}$ , which is lower than the initial limit of  $1200^\circ\text{C}$ , allowed for the bulk W tiles and CFC tiles coated with W for the ILW project in JET [2]. The bulk temperature is measured using thermocouples embedded in tile 5. Figure 4(b) shows the inter-ELM maximum bulk temperature (after subtracting the starting temperature), for an inner, middle and outer position in tile 5 for all low  $\delta$  plasma discharges. The maximum temperature at the outer position of tile 5 is reduced by  $\approx 15\% - 20\%$  for the cases where the strike point is swept to tile 6 and by  $\approx 10\%$  for the case where the strike is swept within tile 5. Similar results have been obtained for the high  $\delta$  plasmas. Sweeping at 4Hz over two sections is enough to reduce the tile bulk temperature to values below the limit envisaged for the ILW.

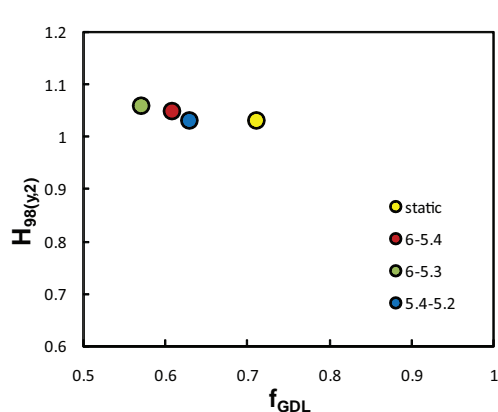


Figure 5: Confinement enhancement factor vs. Greenwald fraction for unfuelled plasmas for the static and swept discharges.

#### 4. Pedestal parameters and plasma performance

It is important that the H-mode performance does not degrade while sweeping the divertor strike points to control the maximum temperature and heat flux on the divertor tile. The plasma confinement enhancement factor is similar for both the static and the swept cases ( $H_{98} \approx 1$ ) as shown in figure 5. The variation in Greenwald fraction observed for the different sweep amplitudes is correlated with the proximity of the outer strike point to the opening of the divertor cryo-pump as it moves on tile 6. In this case, the neutral pumping improves, decreasing the plasma average density. For sweep amplitudes within tile 5 the pumping capacity is reduced, hence an increase of the plasma average electron density is observed. In

conclusion, for the low  $\delta$  configuration, it is possible to reduce the divertor tile surface and bulk temperatures by strike-point sweeping keeping good plasma performance even for the case where the sweep is within tile 5. A similar analysis is ongoing for the high  $\delta$  configuration. The low delta configuration at JET typically shows a degradation of confinement with fueling [9]. To assess if this behaviour is still observed while sweeping, a gas scan is performed for the low delta plasmas using sweep 2.

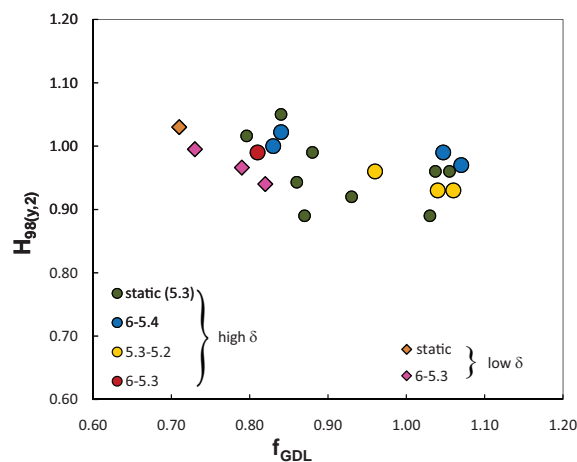


Figure 6: Confinement factor vs. Greenwald fraction for gas scans at low  $\delta$  plasmas sweep 2, and high  $\delta$  plasmas static and swept configurations.

to 0.95 are not accessible. In this case, the unfuelled plasmas already have a Greenwald fraction close to one ( $H_{98}=0.95$ ). Sweeps with smaller amplitude where the outer strike point moves into tile 6, closer to the divertor cryo-pump, can access similar density regions as the static configuration, also obtaining similar confinement.

In conclusion, for the configurations tested in this paper on present CFC divertor tiles, it is possible to sweep the outer divertor strike point over a region compatible to spreading the heat load over two stacks in the bulk W divertor foreseen for the ILW. Measurements of the CFC tiles show a reduction in surface and bulk temperatures compatible with the limitations envisaged for the bulk W tile whilst maintaining good overall plasma performance.

## References

- [1] J Pamela, J. Nucl. Mater 363-365 (2007)
- [2] V Riccardo, 12th International Workshop on Plasma-Facing Materials and Components for Fusion Applications, Julich, Germany, (2009)
- [3] Y. Liang et al. Physical Rev. Letters 98, 265004 (2007)
- [4] F. Sartori et al. 35th EPS Conference, Crete, Greece (2008)
- [5] G Maddison et al., this conference
- [6] P Monier-Garbet, NF 45 (2005) 1404
- [7] M Keilhacker et al., Plasma Phys. Control. Fusion 37 (1995) A3-A17
- [5] S Jachmich et al., this conference
- [9] G Saibene et al., NF 39 (1999) 1133